



## Soot quantification during bio-oil thermal conversion

Y. Chhiti <sup>(1)\*</sup>, R. Ouladsine <sup>(2)</sup>, M. Kemiha <sup>(3)</sup>, M. Bensitel <sup>(4)</sup>

<sup>(1)</sup>Laboratoire LabSIPE, Ecole Nationale des Sciences Appliquées, Université Chouaib Doukali, Eljadida, Maroc

<sup>(2)</sup>Université International de Rabat, Technopolis Rabat, Rabat, Maroc

<sup>(3)</sup>Laboratoire de Biotechnologies Végétales et EthnoBotanique, Faculté des Sciences de la Nature et de la Vie, Université de Bejaia, Algérie

<sup>(4)</sup> Laboratoire de catalyse et de corrosion des matériaux, Université Chouaib Doukali, Eljadida, Maroc.

Received 02 Apr 2016, Revised 02 May 2016, Accepted 03 May 2016

\*Corresponding author. E-mail: [chhiti.younes@gmail.com](mailto:chhiti.younes@gmail.com)

### Abstract

This work investigated the quantification of soot in the producer gas during bio-oil thermal conversion process. A Laser extinction device was specially developed based on Beer-Lambert law. A calibration of the measurement was performed with acetone as one of the model compounds of bio-oil. The pyrolysis of acetone revealed a maximal soot production at 1200°C, at this temperature the model was developed based on the soot volumetric fraction and extinction coefficient. Three sets of experiments were carried out under a large range of temperature (from 1000 to 1400°C) and under different atmospheres: inert atmosphere (pyrolysis), excess of steam (gasification) and with presence of oxygen (partial oxidation). The results showed that temperature and gasifying agents were strong influence on the soot formation and oxidation mechanisms.

**Keywords:** Soot, bio-oil, thermal conversion

### 1. Introduction

The chemistry of soot is a very complex process implying homogeneous and heterogeneous reactions. Soot particle is carbon solid emitted from combustion systems when the local environment is rich enough in fuel which causes incomplete combustion. Soot can represent a problem during the functioning of the engines because it can produce solid deposits, for example in engines with valves [1].

Soot have significant environmental impact and it's an important pollutant itself as a fine particle and consequently breathable. Also, due to its structure, it can act as a condensation core of polyaromatic hydrocarbon (PAHs) and other chemical substances [2]. Aside from its negative effect, it has been proven that soot acts as a significant NO<sub>x</sub> reducing agent [3].

In some cases, the production of soot is highly desirable in furnaces and combustion chamber in order to promote heat exchanges due to the high radiation power of soot, which behaves like a black body and also soot may decrease the rates NO in smoke. But soot particles must be removed before the evacuation of smoke in the atmosphere.

Soot formation has been hardly studied recently in various combustion devices, like flow reactors, shock wave reactors, flame generation device and using different fuels as soot precursors, such as diesel fuels, methane propane and other hydrocarbons [4-7], but the literature on soot formation from biomass remains poor.

A number of issues still remain because of the complexity of soot formation mechanisms.

In parallel with the great progress that has been conducted concerning the determination of its chemical and physical property, many gray areas remain unknown about nucleation, growing and reduction under different operating conditions (temperature, pressure, oxidant agents...). Especially the formation of soot involves many complex chemical and physical phenomenons governing the conversion of the gas fuel in fine solid particles that are not well known at the present time.

The most accepted theory which describes the formation of soot is that advanced by Haynes and Wagner [8], in which the conversion of fuel produces light hydrocarbon, especially acetylene which is considered the main precursor. The first phase is the formation of the first aromatic nuclei by from the aliphatic hydrocarbons species followed by the addition of alkyl species and many other aromatic compounds to provide heavy molecules for example PAHs. These PHA continues to grow until the generation of tiny soot particle with an atomic mass of about 500–2000 uma and with diameters around 1nm [1]. The formation of PAHs appears as an attractive issue to understand the mechanisms of soot formation. The HACA (H<sub>2</sub> abstraction, C<sub>2</sub>H<sub>2</sub> addition) is one of the interesting routes [9, 4], even if there are some other different theories for PAHs growth and soot formation [10].

During its formation and also once soot is formed, it can react with several gases such as O<sub>2</sub>, CO<sub>2</sub> or H<sub>2</sub>O and be gasified. The soot reactivity to these gases is directly related to its structure and composition. Properties such as surface area, particle size and crystallinity affect soot particles reactivity. Soot nanostructure depends on its formation conditions, like fuel origin, residence time and temperature. An understanding of these dependences is fundamental to control the physical properties of the soot and therefore, its chemical reactivity [11-14].

Once soot is formed or even during its formation, it can react with its gaseous environment as O<sub>2</sub>, CO<sub>2</sub> or H<sub>2</sub>O and be gasified. The composition and structure are two key parameters of the reactivity of soot with the gasifying agents. Also, particle size, crystallinity and surface area, affect soot particles reactivity. The nanostructure of soot depends mainly on the operating conditions of its formation, like temperature, residence time and fuel origin. The understanding of these dependences is crucial for to control the chemical reactivity of soot and its physical properties [11-14].

## 2. Materials and methods

### 2.1. Feedstock

The feedstock used for all experiments was bio-oil produced by fast pyrolysis of mixture of hardwood (oak, maple, ash) in an industrial-scale fluidized bed unit (Dynamotive, West Lorne, Ontario) and provided by CIRAD, France. Its fundamental properties are given in Table 1.

**Table 1:** Ultimate and proximate analysis of hardwood derived bio-oil

Ultimate analysis (wt.%)				H <sub>2</sub> O	Ash	Solids	LHV	Kinematic viscosity
C	H	O	N	(wt.%)	(wt.%)	(wt.%)	(MJ/kg)	at 20°C (mm <sup>2</sup> .s <sup>-1</sup> )
43	7,0	50,6	< 0,10	26,0	0,057	2,35	14,5	103

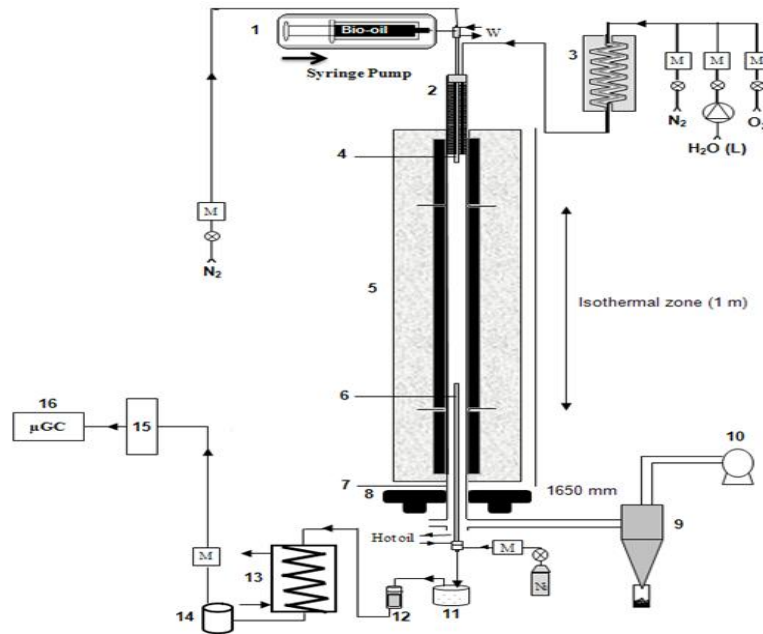
### 2.2. Description of experimental device

The bio-oil thermal conversion experiments were carried out in a continuous flowing system using an Entrained Flow Reactor (EFR) under atmospheric pressure (Figure 1).

The atmosphere gas (15 NL.min<sup>-1</sup>) was preheated at 900°C before being injected in the isothermal zone (reaction zone). Bio-oil is injected inside the reactor thanks to a spray feeder. Bio-oil flowrate of 0.3 g.min<sup>-1</sup> is supported by 3.5 NL.min<sup>-1</sup> N<sub>2</sub> flowrate to ensure a better and uniform spray of bio-oil in the EFR. The injected atmosphere gas flowrate and the sampled gas flowrate were accurately measured using mass flow meters/controllers. The soot in the producer gas are measured by the developed Laser extinction device.

### 2.3. Soot quantification device

Laser extinction was used to make quantitative measurements of soot content in the produced gas. The setup is shown in Figure 2. For laser extinction, a modulated 50kHz, 0.5mW, HeNe laser beam (632.8 nm) is passed through sooting region (optical path of 75 mm) and collected by an integrating sphere, narrow band pass filter, and a photodiode. This collection system accounts for beam-steering effects caused by refractive index gradients and minimizes background interference from soot luminosity [15, 16]. The laser system is aligned so that the light falls on the photodetector system which has two signal outputs. Transmission is measured by splitting the laser beam at the entrance to instrument (beam splitter shown in Figure 3), and using a first photodetector to serve as a laser power reference. The rest of the beam passes through the sooting region. When light passes through a soot particle, part of the light energy is absorbed by the atoms. The amount of the absorbed light depends on the characteristics of the soot and the sooting region thickness.



- |                              |                          |
|------------------------------|--------------------------|
| 1- Syringe pup               | 9- Cyclone collector     |
| 2- preheater                 | 10- Exhaust ventilator   |
| 3- Vapour generator          | 11- Hot settling box     |
| 4- spraying feeder           | 12- Filter               |
| 5- furnace                   | 13- Water cooler         |
| 6- sampling device           | 14- Condensate collector |
| 7- alumina reactor           | 15- Gas dryer            |
| 8- Soot quatification device | 16- Gas analyser         |

**Figure 1 :** Schematic setup of the Entrained Flow Reactor (EFR)

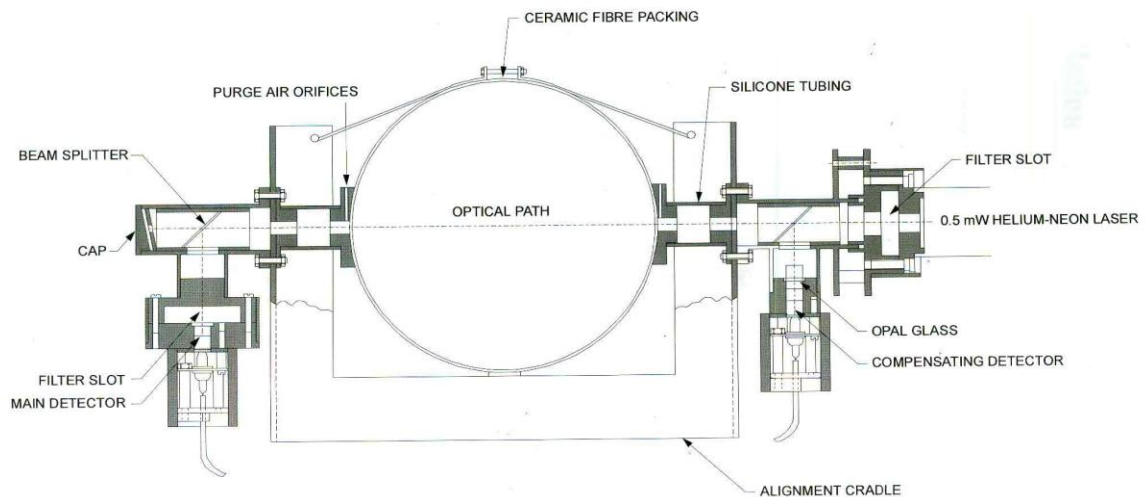


**Figure 2:** Schematic representation of the optical setup for soot quantification

The transmitted laser intensities  $I$  and  $I_0$  with and without soot, respectively, are related to optical thickness  $L$  through the relationship Eq. 1:

$$K = \ln(I_0/I)/L \quad (1)$$

Where  $K$  is the extinction coefficient. The above intensities were corrected for background luminosity by turning off the modulated laser.

The optical thickness can be quantitatively related to the soot volumetric fraction through a linear relation [17-20]. The coefficient associated to this relation was experimentally determined, as explained below.

### 3. Results and discussions

#### 3.1. Soot quantification methodology

Bio-oil contains a large amount of water (26%), and during pyrolysis, a considerable amount of condensate species (tar+water) is produced. These species tend to condensate on the soot particles and make therefore soot become sticky. Hence the weighing of the soot collected in the sampling probe and in the filter is difficult. To face with this issue, a calibration of the measurement was performed with acetone. Acetone is considered as one of the model compounds of bio-oil. Moreover, as shown in the SEM observations of Figure 3, the soot produced by acetone and the ones produced by bio-oil have very similar size in the range of 10 to 50 nm. Chain aggregates are composed from several tens or more of sub-units, known as spherules or monomers, can be observed in both cases.

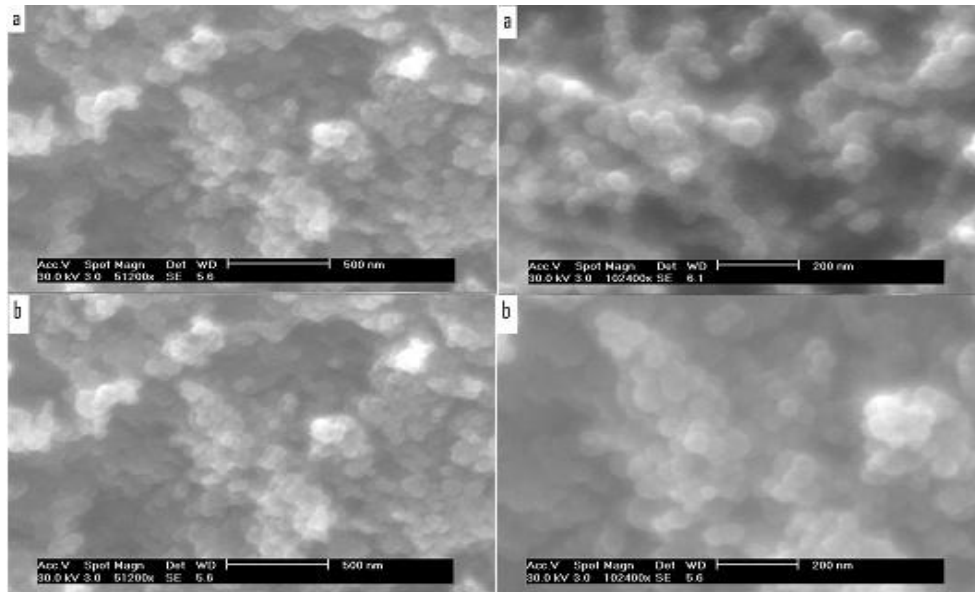


**Figure 3:** SEM images of the soot particles samples obtained from acetylene and from bio-oil pyrolysis at 1200°C. **a** - acetone; **b** - bio-oil

The acetone was pyrolyzed at different temperatures ranging from 1000 to 1400°C. Figure 4 shows the extinction coefficient measured at different temperatures. It shows that a maximum of soot is produced at 1200°C. This temperature was chosen for further calibration. Extinction coefficient values in this sooting condition exceeded 6 m<sup>-1</sup>. At this temperature, there are black clouds of soot moving and floating along the reactor; the opacity of the clouds makes the nozzle invisible from the bottom of the reactor.

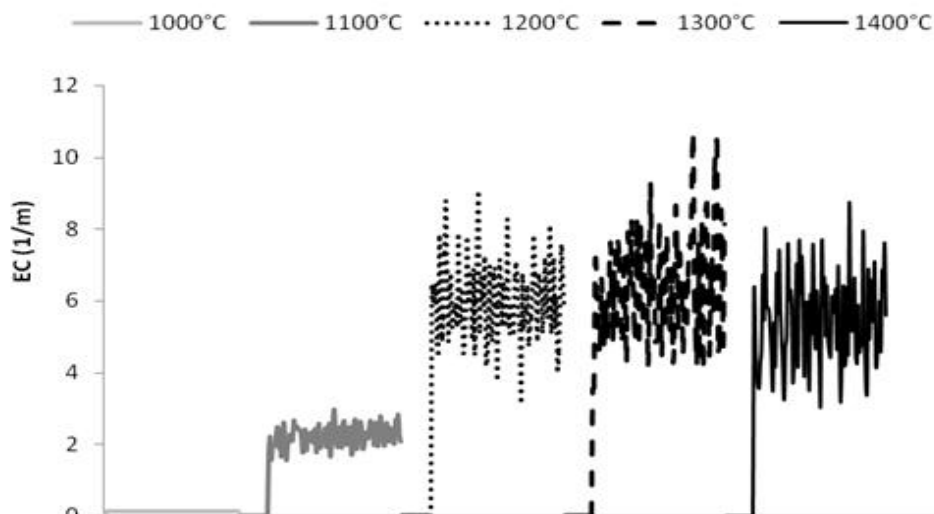


**Figure 4.** Extinction coefficient versus temperature – acetone pyrolysis

The pyrolysis of acetone was also carried out using different flow rates of acetone: 6, 12 and 18 ml/h. For each experiment the EC was continuously measured, as shown in Figure 5. Each experiment was then repeated with the laser device off and the sampling probe set in. After pyrolysis, soot in the sampling probe, in the settling box and in the filter was collected and accurately weighed. The soot volumetric fraction was calculated for each experiment using the relationship Eq. 2:

$$F_v = \frac{\text{Soot volumetric flow rate}}{\text{Total volumetric flow rate}} = \frac{Q_{m_s}/\rho_s}{Q_{v_g} \cdot \frac{T}{273}} \quad (2)$$

With

$F_v$	Soot volumetric fraction
$Q_{m_s}$	Soot mass flow rate (g/min) = mass of soot/sampling time
$\rho_s$	Soot density = 1800 g/l
$Q_{v_g}$	Nitrogen volume flow rate sweeping the reactor (NL.min <sup>-1</sup> )
$T$	Temperature (°C)

The total gas flowrate at the exit of the reactor was calculated based only on the N<sub>2</sub> flowrate fed to the reactor assuming that the fraction of produced gas and soot is negligible.

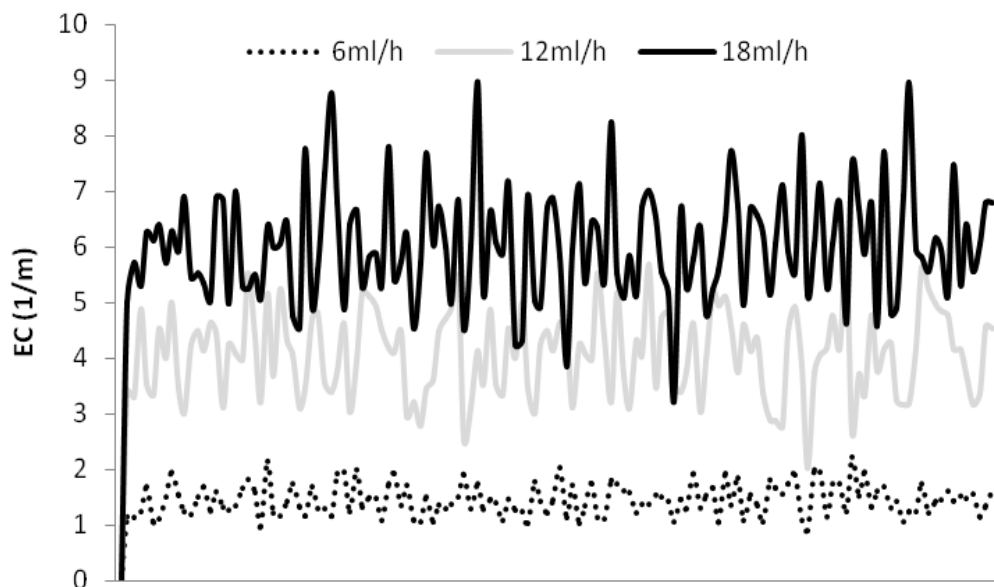


**Figure 5:** Extinction coefficient during acetone pyrolysis at 1200°C with different acetone flowrates

Figure 6 shows the calculated volumetric fractions (in ppb) versus the measured EC. The obtained calibration curve is a linear function ( $F_v = s \cdot EC \cdot 10^{-9}$ ) with a slope of  $s = 16.89$ . This factor is subsequently used for all experiments to derive the mass yield of soot following Eq. 3:

$$\text{Yield} = \frac{Q_{v_g} \cdot T \cdot s \cdot EC \cdot 10^{-9} \cdot \rho}{273 \cdot Q_{m_{B,O}}} \quad (3)$$

With:  $Q_{m_{B,O}}$  bio-oil mass flow rate (g/min).

One should note that the value for  $\rho_s$  fixed at 1800g/l is used twice in the calculations and has finally no impact on the calculated soot mass yield.

Note that the presence of char during the quantification of soot may impact the measurement. Previous studies have shown that the char yield during pyrolysis process is lower than 1% of the initial bio-oil at 1000°C and still lower at higher temperature. At 1000°C, the laser detects almost nothing (yield < 0.1%). This is reassuring for soot measurements in the temperature range of 1000-1400°C explored in this work.

### 3.2. Soot production during bio-oil conversion

The operating temperature was varied over the range of 1000-1400°C. Gas atmosphere was preheated at 900°C for all experiments. Bio-oil was then continuously fed by a feeding probe and injected into the reactor tube through a nozzle by a nitrogen stream. The feeding rate of feedstock was of 0,3 g/min, as explained previously.

- Firstly, the simplest situation of pyrolysis: i.e. in an inert atmosphere was studied. In this case, the reactions involved are devolatilization, cracking, and some reforming and gasification by H<sub>2</sub>O that is present in the fed bio-oil.
- Secondly excess of H<sub>2</sub>O, called steam gasification was studied. Gasification tests were carried out by supplying a mixed stream of nitrogen with steam. The steam to carbon molar ratio was S/C= 8.3 which was equivalent to 10 vol. % of steam in the atmosphere gas.
- Lastly the presence of O<sub>2</sub> was explored. The so called partial oxidation tests were carried out by supplying a mixture stream of nitrogen with O<sub>2</sub>. The amount of O<sub>2</sub> was varied from very small amount to investigate a potential impact through radicals (O/C= 0.075), to large amount that may oxidize a significant part of bio-oil (O/C=0.5). This is equivalent to 0.1-0.75 vol. % of oxygen in atmosphere gas.

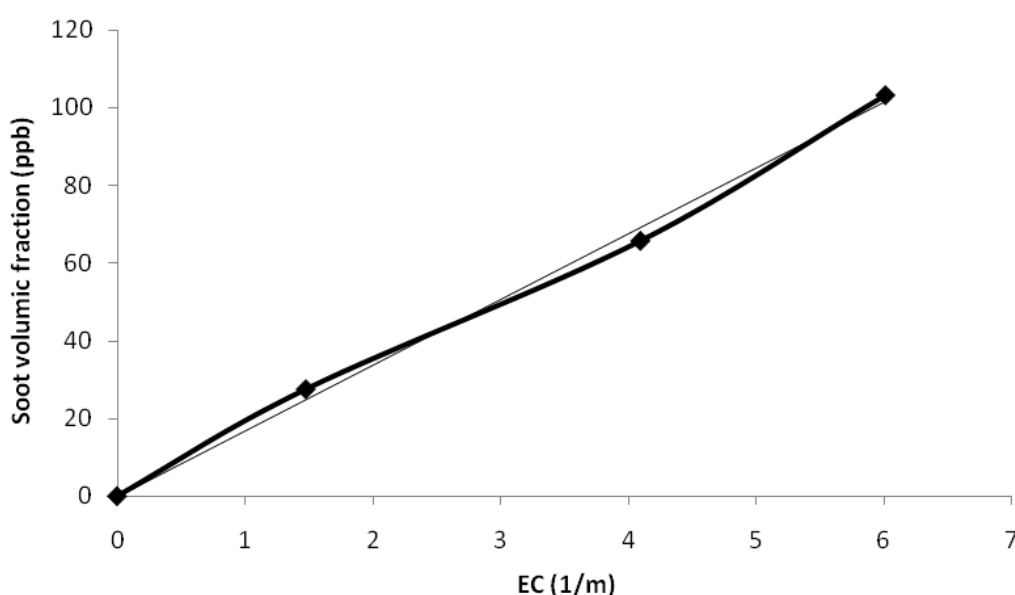


**Figure 6 :** Soot volumetric fraction versus extinction coefficient

The results of soot yields obtained in the different experiments of pyrolysis, gasification, and partial oxidation are shown in Figures 7-a, 7-b and 7-c respectively. These figures show both the response of the laser and the yield obtained by the method developed.

In the case of pyrolysis (Figure 7-a), an increase in temperature results an increase in the soot yield. The absence of any oxidizing agent and the increasing of temperature favor the formation of the precursors as PolyAromatic Hydrocarbons (PAH) and subsequently soot formation [8].

In the gasification case, the soot yield is more than 3 times smaller than the soot yield in the pyrolysis case, as can be seen in Figure 7-b. The curve is bell-shaped. At 1000°C curve shows a low soot yield, which gets higher when reaction temperature increases and until the soot yield reaches a maximum of  $1.27 \cdot 10^{-2}$  g/g at about 1200°C. Above 1200°C, the soot yield strongly decreases. This decrease may be explained by steam and CO<sub>2</sub> gasification of soot.

In the partial oxidation situation the O/C molar ratio was varied from 0.075 to 0.5 at 1200°C, as can be seen in Figure 7-c, the measured amount of soot strongly decreases with the O/C ratio under the conditions explored. According to the literature, when O/C molar ratio increases, most hydrocarbons are broken by thermal decomposition or oxidation, and several intermediate species are formed. In this case, a competition between oxidation reactions and the molecular growth occurs. Oxidation reactions lead to the formation of various oxygen-compounds intermediates and products like CO<sub>2</sub>, CO and H<sub>2</sub>O. As a result, the soot production decreases compared with the case of pyrolysis.

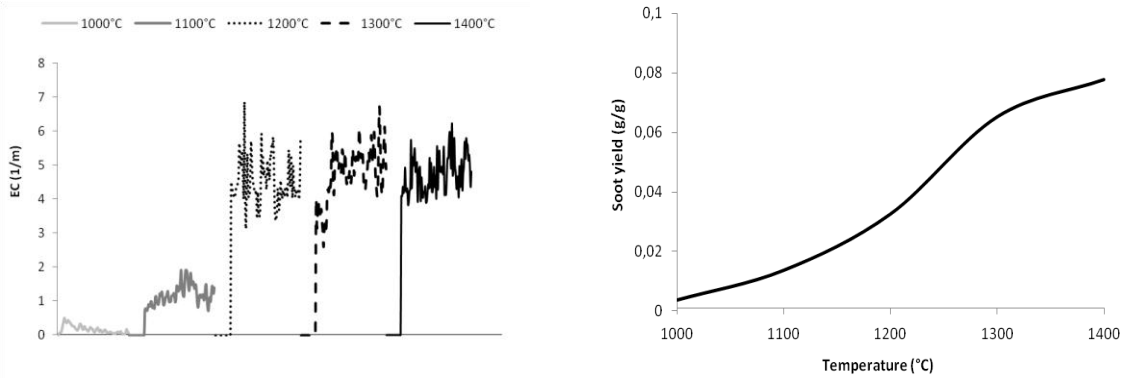


**Figure 7-a:** Soot yields versus temperature: pyrolysis case

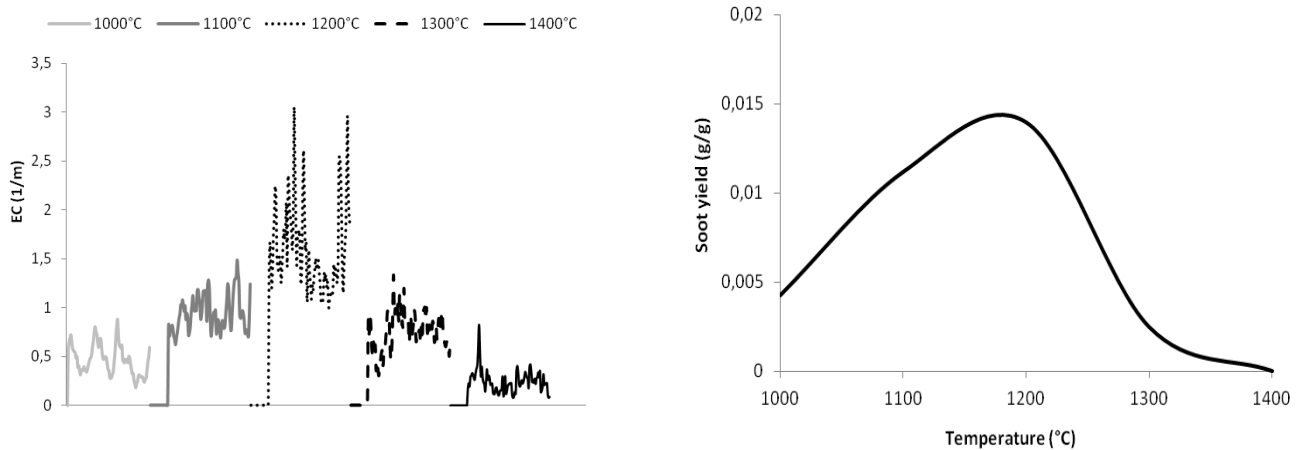


**Figure 7-b:** Soot yields versus temperature: gasification case

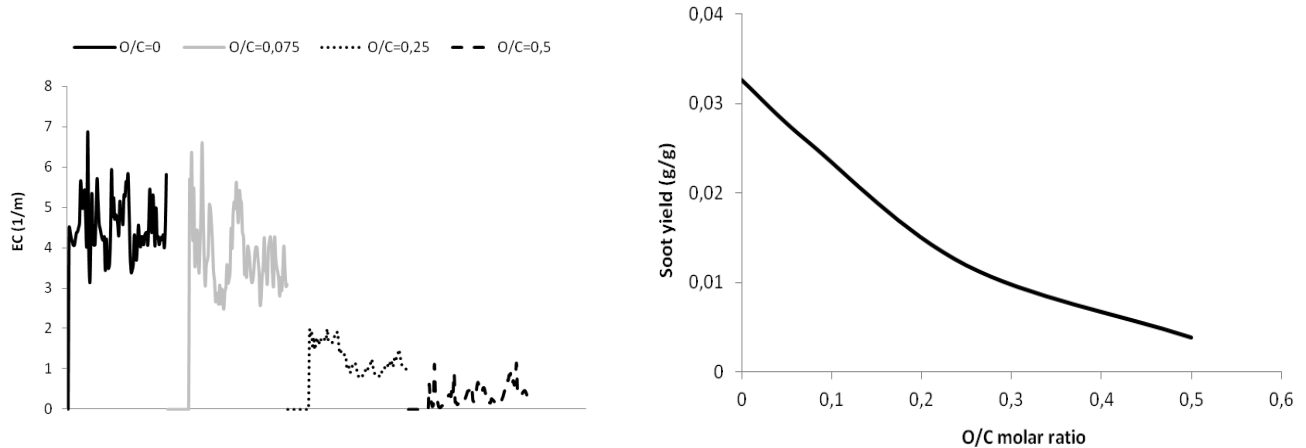


**Figure 7-c:** Soot yields versus O/C molar ratio at 1200°C: Partial oxidation case

## Conclusion

A Laser extinction device based on Beer-Lambert law was specially developed to quantify Soot production during bio-oil thermal conversion in an entrained flow reactor. A calibration of the measurement was performed with acetone as one of the model compounds of bio-oil. The pyrolysis of acetone revealed a maximal soot production at 1200°C, at this temperature the model was developed based on the soot volumetric fraction and extinction coefficient.

Soot quantification method developed in this work allows to accurately measuring the soot yield during bio-oil thermochemical conversion. The experimental results showed that an increase in temperature favors the soot formation during pyrolysis process. In the gasification case, the soot yield increase until an optimum at 1200°C, after which it strongly decreases. However the soot amount strongly decreases with the O/C ratio in the partial oxidation situation.

## References

1. Bozzano G., Dente M., Faravelli T., Ranzi E., *Processes Appl. Therm. Eng.* 22 (2002) 919.
2. Ambrogio M., Saracco G., Specchia V., Gulijk C., Makkee M., Moulijn J.A., *Sep. Purif. Technol.* 27 (2002) 195.
3. Bilbao R., Millera A., Alzueta M.U., *Ind. Eng. Chem. Res.* 33 (1994) 2846.
4. Frenklach M., Wang H., *Springer Verlag, Heidelberg.* (1994) 165.
5. Richter H., Howard J.B., *Prog. Energy Combust. Sci.* 26 (2000) 565.
6. Skjøth-Rasmussen M.S., Glarborg P., Østberg M., Larsen M.B., Sørensen S.W., Johnsson J.E., Jensen A. D., Christensen T.S. *Proc. Combust. Inst.* 29 (2002) 1329.
7. Skjøth-Rasmussen M.S., Glarborg P., Østberg M., Johaneessen J.T., Livbjerg H., Jensen A.D., Christensen T.S., *Combust. Flame.* 136 (2004) 91.
8. Haynes B.S., Wagner H.G., *Prog. Energy Combust. Sci.* 7 (1981) 229.
9. Frenklach M., *Chem. Chem. Phys.* 4 (2002) 2028.
10. Krestinin A.V., *Combust. Flame.* 121 (2000) 513.
11. Vander Wal R.L., Tomasek A.J., *Combust. Flame.* 136 (2004) 129.
12. Murr L.E., Soto K.F., *Mater. Charact.* 55 (2005) 50.
13. Grieco W.J., J. Howard B., Rainey L.C., Vander Sande J. B., *Carbon.* 38 (2000) 597.
14. Grieco W.J., Howard J.B., Rainey L.C., Vander Sande J.B., *Chem. Phys. Lett.* 194 (1992) 62.
15. Musculus M.P., Dec J.E., Tree D.R., *SAE Paper No.* 2002-01-0889, (2002).
16. Pickett L.M., Siebers D.L., *Proc. Combust. Inst.* 29 (2002) 655.
17. Pickett L.M., Siebers D.L., *International Journal of Engine Research.* 7 (2006) 103.
18. Choi M.Y., Hamins A., Mulholland G.W., Kashiwagi T., *Combust. Flame.* 99 (1994) 174.
19. Cignoli F., DeJuliis S., Manta V., Zizak G., *Appl. Opt.* 40 (2001) 5370.
20. Coppalle A., Joyeux D., *Comb. Flame.* 96 (1994) 275.

(2016) ; <http://www.jmaterenvirosci.com/>